KISHIN MOORJANI

RANDOM MAGNETS

Synthetically structured materials are increasingly dominating the arena of solid-state sciences and technologies. Amorphous materials form an important component of this new and exciting development. This article reviews the basic concepts relevant to amorphous magnetic materials and discusses various dynamical phenomena revealed in recent studies. The results establish a lack of time scale for spin dynamics in random magnets and exhibit a universal temperature dependence of spin relaxation in a large variety of systems with noncollinear magnetic structures.

INTRODUCTION

Magnetic materials play a fundamental role in many of the electrical and electronic systems that characterize modern society. But, as concluded in a recent National Materials Advisory Board report,[1] all major magnetic technologies in the United States are facing a potential problem because our dependence on imports poses serious problems to our economy and national security. The report identifies amorphous magnetic materials, permanent magnets, and magnetic recording as three growth areas and strongly recommends "to regenerate a strong university-based research programs in magnetism and magnetic materials," particularly "in support of those technologies with strong growth potential or having strategic value."

All materials respond to external magnetic fields and, therefore, in principle, are magnetic. But the phrase "magnetic material" is generally reserved for solids that exhibit collective magnetic properties, i.e., materials composed of atoms that possess uncompensated electronic spins and, therefore, magnetic moments that interact via exchange forces and, thus, produce the magnetic properties. These requirements are independent of the atomic structure of a solid. However, until recently, scientific concern as well as technological uses of magnetic materials were focused on those solids where atoms are arranged on an orderly crystalline lattice.

The tyranny of crystalline order imposes severe constraints on the type and relative concentrations of atoms that can be assembled to form alloys with varying physical and chemical characteristics. Recently developed techniques, however, use rapid quenching of vapors or liquids to synthesize solids with disordered atomic structures that can be fabricated over an extended range of concentrations of atoms to form hitherto unknown materials whose properties can be custom-tailored and fine-tuned to suit desired needs. The availability of these materials has ushered in a scientific and technological revolution in condensed matter sciences. The observation that many phenomena are essentially unaltered by the absence of a periodic lattice has forced a reappraisal of the existing theoretical framework. This, combined with the novel phenomena induced by disorder, has set the stage for intense activity in disordered structures. The consequences have been felt far beyond the subject of materials sciences, and the emerging concepts are finding rapid applications in mathematics, with its recent interest in fractals and chaos, and in biology, where structural disorder abounds.

The ease and economy of producting random or amorphous magnetic materials, the subject of the present article, have already found a plethora of industrial applications. The soft magnetic properties of amorphous ferromagnets, related to high permeability arising from the absence of magnetocrystalline anisotropy, have been exploited successfully in electric power distribution transformers that are being operated in various utility companies in the United States and Japan. Other applications range from amorphous metal cores in phonograph cartridges, which provide decreased signal distortion and lower noise than the conventional Permalloy core, to amorphous heads for computer recording equipment, magnetic materials for magneto-optic recording, and permanent magnets. The latter category of high-energy product materials with properties superior to rare and expensive cobalt-based alloys are in fact crystalline (prototype $Nd_2Fe_{14}B$), but were discovered accidentally while adding boron as a glass former to rapidly quenched rare-earth/transition-metal alloys. Conversely, amorphous metals were discovered accidentally while attempting to form crystalline solid solutions; the interplay between crystalline and amorphous materials continues. Novel concepts and techniques, introduced to understand amorphous solids, are finding relevance to phenomena observed in crystalline materials.

The APL activity in amorphous magnetism[2] dates from the birth of the subject approximately 15 years ago. Since then, a great deal of progress has occurred, much of which has been reviewed in a monograph[3] and a review article.[4] In this article, after sketching some salient features of the field, recent advances[5,6] are discussed.

DISORDER-INDUCED EFFECTS

The essential ingredients of long-range magnetic order—magnetic moment and exchange interactions—are both altered by disorder, since the former depends on the immediate chemical environment (number, type, and separation of atoms) of a given atom and the latter is a sensitive function of the interatomic distance. The changes induced by chemical inequivalency of sites and inequivalency of interatomic separation in amorphous solids (Fig. 1) will be considered in turn. The discussion is limited to amorphous alloys, since elemental amorphous magnets pose difficulties of fabrication and since the sparse information available on them is obtained mostly from extrapolation of the data on alloys.

Magnetic Moments

The magnitude of magnetic moment, as established for the studies on crystalline alloys, is determined mainly by the chemical environment. More than one value (but a finite number of values) of the magnetic moment is observed even in crystalline compounds such as Fe_3Si and Fe_2B owing to chemical inequivalency of sites. Disorder, however, can lead to a variety of chemical environments in an amorphous material so that a distribution of moments is induced. The spread in moment distribution can be sufficiently large in some cases for magnetic and nonmagnetic atoms of the same element to coexist. Moments can also be drastically affected, as is seen most vividly in alloys such as a-$Fe_{0.5}Si_{0.5}$ and a-$Co_{0.5}Sn_{0.5}$, which are nonmagnetic in the crystalline state (due to the chemical environment being unfavorable for the existence of a magnetic moment on the transition metal atoms[7]), but become magnetic in the amorphous state (since multiple environments are possible with some of them favoring the formation of magnetic moments[8]). The average moment is determined from the bulk magnetization measurements. Such measurements, however, give no information about either the distribution of moments due to chemical inequivalency of magnetic atoms in an amorphous material, or about the distribution of moments between different types of magnetic atoms. To obtain this local information, one has to use local probes such as Mössbauer or nuclear magnetic resonance spectroscopies. The applications of these techniques to magnetic measurements have been reviewed elsewhere;[3] Fig. 2 shows typical results.[9]

Exchange Interactions

Exchange interactions, whether direct or indirect, depend sensitively on the distance between the interacting electrons. Superexchange via ligands depends additionally on metal-ligand-metal bond angles. Therefore, it is clear that the distribution of interatomic separations in a noncrystalline solid will lead to a distribution of exchange interactions. In iron-based amorphous alloys, the distribution often includes exchange interactions of both signs since the nearest-neighbor Fe-Fe separation in these alloys covers the distances of 2.58 and 2.48 angstroms, corresponding, respectively, to ferromagnetic α-iron and antiferromagnetic γ-iron.[10] Thus, while the probability of finding an exchange interaction of a given magnitude and sign, $P(J)$, consists of one or more delta functions for a crystal, the disorder in an amorphous solid will broaden the peaks, even to the extent of encompassing interactions of both signs in the distribution (Fig. 3). In the framework of

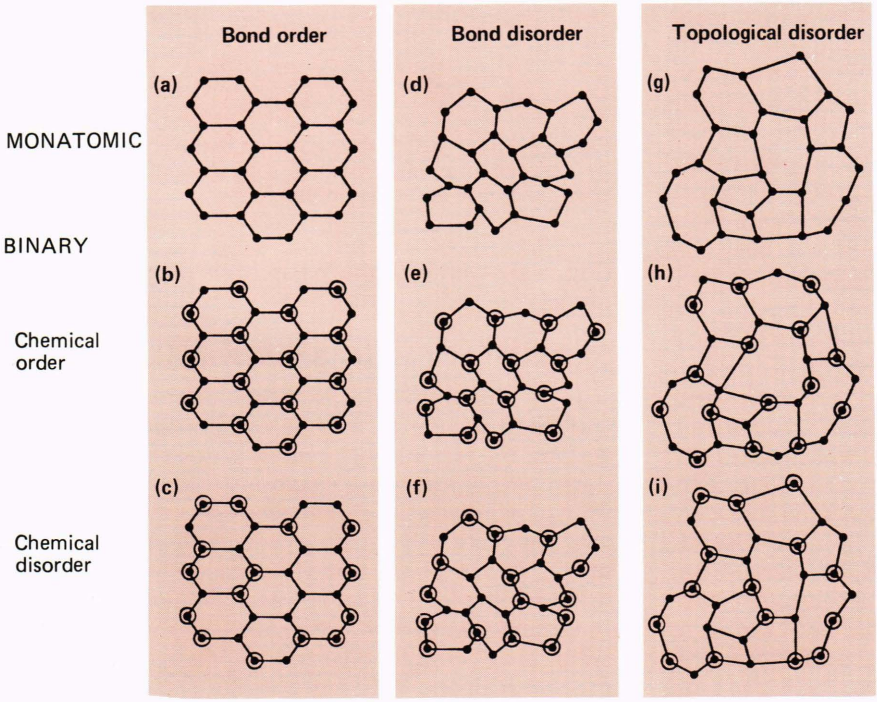

Figure 1—Types of disorder in two-dimensional monatomic and binary atomic structures. The illustrations in the left column show hexagonal lattices: (a) monatomic lattice with bond order, i.e., a single value for bond angles; (b) binary lattice with bond and chemical order, i.e, each atom surrounded by three atoms of the other species; and (c) binary lattice with bond order but chemical disorder. The illustrations in the middle column are obtained from the corresponding ones in the left column by introducing a distribution of bond angles without changing the coordination number; i.e, every atom is still a part of a six-membered ring possessing three nearest neighbors. The illustrations in the right column depict topological disorder where, besides bond disorder, one has 4-, 5-, 6-, 7-, and 8-membered rings.

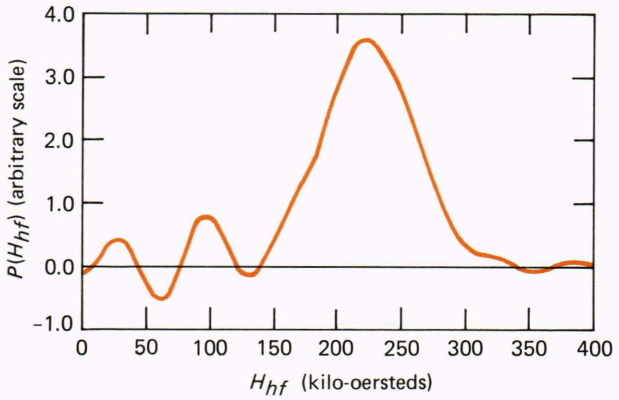

Figure 2—Hyperfine field distribution of sputtered amorphous $Fe_{71}B_{29}$ alloy at room temperature obtained from Mössbauer spectroscopy. The field distribution reflects the distribution of magnetic moments arising from many chemically inequivalent sites in an amorphous material. The oscillations about zero arise from the fitting procedure and are to be ignored.

molecular field approximation applied to amorphous magnets, the magnitude of the effective field will certainly have a probability distribution, but, in all cases except ferromagnets where $P(J)$ is predominantly or exclusively positive, the direction of the effective field will have a probability distribution as well.

The distribution of exchange interactions, unlike that of magnetic moments, cannot be measured directly. Only its effects on magnetic parameters (e.g., the Curie temperature) can be inferred from measurements. We shall return later to this point.

Anisotropy

After exchange, the next most significant factor determining the properties of magnetic materials is single-ion anisotropy. Each atom or ion in a solid experiences an electrostatic field created by the charges of all the other atoms or ions, plus a contribution from any conduction electrons. This electrostatic field, which has the point symmetry of the site in a crystal, tends to lift the degeneracy of the energy levels of partly filled d or f shells. The particular spatial distribution of atomic electron density stabilized by Coulomb interaction with the electrostatic potential is associated with a specific state of orbital angular momentum, and, via spin-orbit coupling, certain preferred directions are then imposed on the atomic magnetic moment. Single-ion anisotropy resulting from electrostatic fields is generally most important for the $4f$ rare-earth series.

The single-ion anisotropy energy can schematically be represented by an energy surface, which in a crystal possesses the same symmetry as the point group of the atomic site (Fig. 4a). In an amorphous solid, however, no such symmetry survives, except for time-reversal, so that the anisotropy energy surface becomes too complex (Fig. 4b) to be amenable to an analytic description. An analytic description can, however, be restored by assuming a random axial anisotropy (i.e., different randomly oriented easy direction at each site)

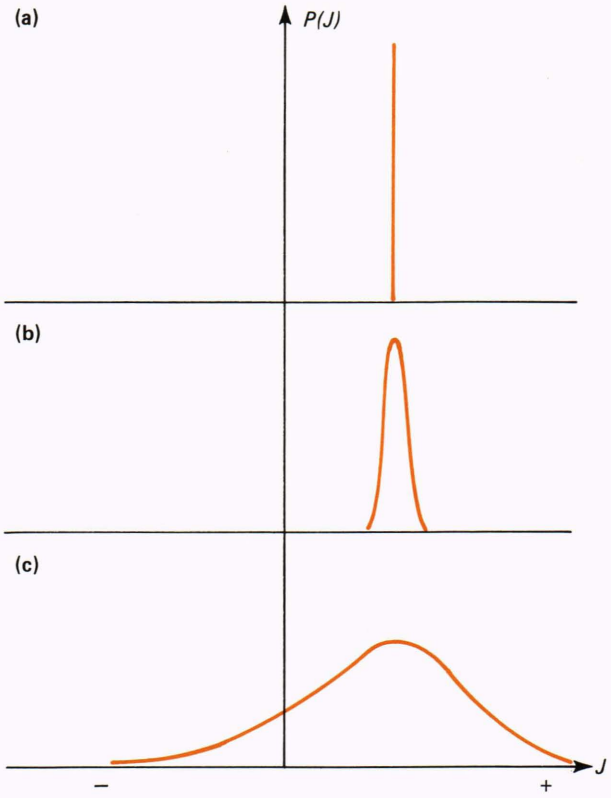

Figure 3—Probability of finding a given value of exchange interaction, J, (a) in a crystal and (b) and (c) in amorphous solids with different amounts of disorder.

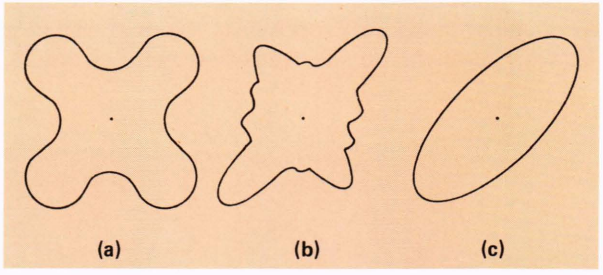

Figure 4—Schematic representation of the anisotropy energy surfaces for a single ion in (a) a crystal, (b) an amorphous solid, and (c) a particular model.[11]

(Fig. 4c), which is the basis of a much-celebrated model.[11]

FERROMAGNETIC EXCHANGE

If the distribution of exchange interaction is wide enough to encompass enough antiferromagnetic interactions, the ferromagnetic phase is unstable and a random noncollinear phase results instead. But even when only ferromagnetic exchange exists, it is not clear whether there still will be a well-defined Curie point at T_c, i.e., a phase transition characterized by the usual scaling laws. It is, however, intuitively obvious that the extent to which the nature of the phase transition is affected by disorder will depend on the degree of disorder. Whether disorder is in the form of

dilution caused by missing magnetic bonds or sites, or fluctuations in the magnitude of J, it will tend to induce local spatial fluctuations, ΔT_c, in the ordering temperature that, if large enough, can actually destroy the phase transition. Quantitative limits can be obtained as summarized below.

An essential characteristic of a continuous phase transition is the rapid divergence in correlated behavior as one approaches T_c from above. In particular, the correlation length, ξ, grows as $|T - T_c|^{-\nu}$, a relationship that defines the critical exponent, ν. Imagine the situation in a disordered magnetic material where independent volumes of approximate dimensions ξ^3 can be defined with local T_c's within a band ΔT_c. As the temperature is reduced, these volumes will grow. However, the neighboring regions can only continue to grow without mismatch if they have T_c's so that ΔT_c is less than $|T - T_c|$. Quantitative analysis of the argument imposes a limit on ν for a sharp transition. But since it is not ν but thermodynamic quantities such as specific heat that are most easily measured, one obtains limits on α, the specific heat exponent [$C \approx (T - T_c)^{-\alpha}$, $T > T_c$] via the scaling relation $\alpha = 2 - d\nu$, d being the dimensionality. A sharp transition is found[12] for the diluted bond problem in three dimensions only if $\nu > 2/3$ (i.e., $\alpha < 0$). For $\alpha > 0$, the width of the temperature range over which the rounding effect on the phase transition occurs is estimated to be $\Delta T/T_c \approx x_b^{1/\alpha}$, where x_b is the concentration of missing bonds. Similarly for amorphous ferromagnets, $\Delta T/T_c \approx (\delta J/J)^{2/\alpha}$, where $\delta J/J$ is the relative fluctuation in J.

Experimentally, well-defined T_c's and sharp phase transitions have been observed for a large number of homogeneous alloys.[3] The data on T_c for amorphous alloys, when extrapolated to pure metals, show that cobalt-based alloys differ considerably from the iron-based ones. While the value of T_c for amorphous cobalt is close to that for hexagonal close-packed cobalt, that for amorphous iron is roughly one-third the value for body-centered cubic iron. This is because of the presence of some iron-iron pairs that interact antiferromagnetically and hence rapidly depress T_c.

The overall temperature dependence of magnetization has been measured for a number of amorphous ferromagnetic alloys; some typical examples are shown in Fig. 5, where they are also compared with the curves for two crystalline materials. Notice that the reduced magnetization versus reduced temperature curves for amorphous alloys lie substantially below those for crystalline iron. However, such an effect is not unique to magnetic glasses but has also been observed for crystalline Invar alloys (Fig. 5). Although no complete theoretical understanding of this behavior exists, a number of effective field approaches do produce the overall features. Any fluctuations in J reduce T_c and depress magnetization compared to those for the mean crystal.[13-15]

In crystalline ferromagnets, the reduction in low-temperature magnetization with increasing temperature is caused by the thermal excitation of long wavelength

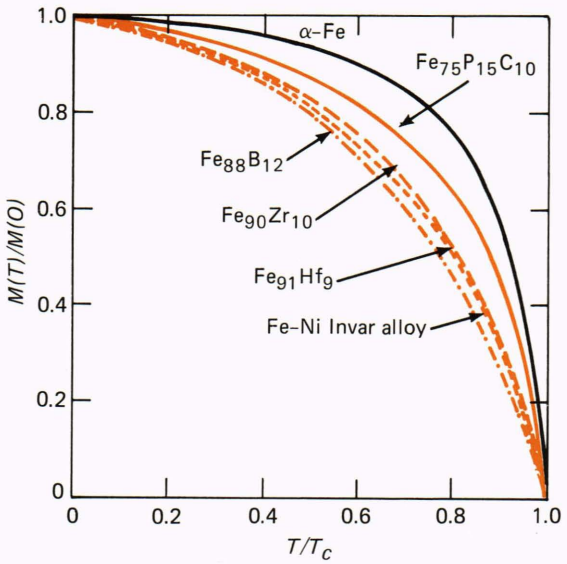

Figure 5—Comparison of reduced magnetization curves for α-Fe, a crystalline Invar alloy, and a number of amorphous alloys. Note that the curves for alloys show values of reduced magnetization that are depressed with respect to the value for α-Fe.

spin waves that, in the absence of Brillouin zone effects, obey the dispersion relation, $E(q) = Dq^2$, where q is the wave vector, $E(q)$ is the energy of the noninteracting spin waves, and D is the stiffness constant. The resulting effect of the spin waves on $M(T)$ is given by $M(T) = M(O)\,(1 - BT^{3/2})$, and the coefficient B and the stiffness constant D in the linear spin wave theory are related by

$$B = \frac{\zeta(3/2)g\mu_B}{M(O)} \left(\frac{k}{4\pi D}\right)^{3/2}, \qquad (1)$$

where ζ is the zeta function, g denotes the g factor, μ_B denotes the Bohr magneton, and k is the Boltzmann constant.

Although the above results for long wavelength spin waves were first obtained by Bloch[16] using the Heisenberg hamiltonian for spins on a lattice, the quadratic dispersion relation has been shown to possess a far more general validity and is appropriate even for a continuous magnetic medium.[17] Once the quadratic relationship is assumed, the $T^{3/2}$ dependence of magnetization follows even in the absence of crystalline structure. At low temperatures, only a few spin waves are excited so that they can be treated as bosons. Their number, n, is the phase volume divided by the volume of a unit cell and is equal to $(4\pi/3)(hq)^3/(2\pi h)^3$, so that n is proportional to q^3. But since the dispersion relation implies that $Jq^2 \approx T$, n is proportional to $(T/J)^{3/2}$, and therefore to $(T/T_c)^{3/2}$. It is thus not surprising that the Bloch $T^{3/2}$ law is found for amorphous ferromagnets and that the existence of long-wavelength spin waves has also been inferred from inelastic neutron scattering and ferromagnetic resonance experiments as well as measurements of the hyperfine field. The $T^{3/2}$ behavior of the magnetization was first reported in a-Co_xP_{100-x} alloys;[18] subsequently,

similar behavior has been reported in many other amorphous alloys. Distinct differences, however, are seen relative to crystalline ferromagnets. The $T^{3/2}$ variation of magnetization in amorphous alloys (Fig. 6) persists from 0.2 to $0.5T_c$, which is a much larger temperature range than is observed in crystalline ferromagnets, where deviations from $T^{3/2}$ behavior begin to dominate beyond $1.5T_c$. Furthermore, the value of the coefficient B for amorphous alloys is a few times larger than the value in crystalline ferromagnets having similar Curie temperatures, showing the relative ease with which spin waves are excited in amorphous ferromagnets.

It should be noted that the first confirmation of surface spin waves[20] has come from the electron scattering studies on the amorphous alloy $Ni_{40}Fe_{40}B_{20}$. Surface spin waves giving the same $T^{3/2}$ dependence of magnetization as the bulk spin waves but with the value of coefficient B twice that for bulk spin waves had been predicted from analysis of the Heisenberg model.[21] They had escaped detection because of the inability to separate bulk and surface contributions to magnetization. In amorphous alloys, diffraction effects from the bulk are eliminated, thereby facilitating the observation of asymmetry in the elastic scattering of spin-polarized electrons from the surface atomic layers only. A $T^{3/2}$ dependence of surface magnetization was found experimentally,[20] but the value of coefficient B is 1.5 times that predicted theoretically.[21]

COMPETING EXCHANGE

The competing exchange interactions and the resulting noncollinear magnetic structure were initially postulated to explain a sharp cusp in the low-field alternating-current magnetic susceptibility of dilute noble-metal/transition-metal alloy AuFe in the concentration range of 1 to 22 percent Fe.[22] The cusp occurs at temperatures where Mössbauer studies had previously shown the appearance of some sort of magnetic order evidenced by a magnetic hyperfine field,[23] and neutron scattering data had ruled out any long-range antiferromagnetic order.[24] The possibility of a thermodynamic phase transition to a random magnetic structure, spin glass, was therefore envisaged.[25] The analysis was based on a model that included random exchange interactions of either sign, since the predominant exchange in noble-metal/transition-metal alloys is the Rudermann-Kiltel-Kasuya-Yosida (RKKY) interaction, which oscillates as a function of interimpurity separation. Since then, an entire industry has blossomed around the spin glass subject.[26] A large number of crystalline and amorphous alloys, both insulating and metallic, and dilute as well as concentrated, show the signatures that have come to be associated with the transition to the spin glass state. In the process, a number of novel concepts have emerged that we will discuss briefly.

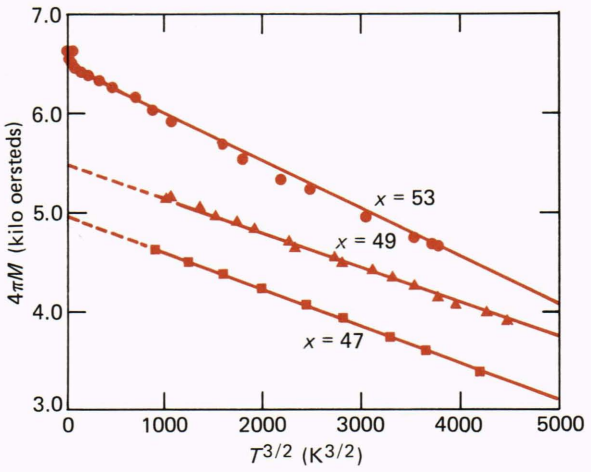

Figure 6—The $T^{3/2}$ temperature dependence of the magnetization deduced from ferromagnetic resonance data on amorphous Fe_xB_{100-x} alloys, showing the existence of long-wavelength spin waves in amorphous magnets. Below 80 K, x = 47 and 49 alloys do not show a simple behavior due to a transition to a noncollinear magnetic phase (see Fig. 10), hence, the dashed lines.[19]

Frustration and Spin Glasses

We will first consider a particularly useful concept termed frustration.[27] In magnetic solids, it arises either from the conflict caused by the simultaneous presence and ensuing competition between ferromagnetic and antiferromagnetic exchange interactions or from the presence of antiferromagnetic interactions in an amorphous structure. It has been fruitfully applied to the study of ground state and low-lying excited states of spin glasses.

Consider Ising spins, $S_i = \pm 1$, at the corners of a square interacting via nearest-neighbor exchange interaction, J_{ij}. *For* $J_{ij} > 0$, one obtains the ferromagnetic configuration (Fig. 7a) of spins and, for $J_{ij} < 0$, the antiferromagnetic configuration results (Fig. 7b). Both of these configurations have the ground state energy $-4J(J_{ij} = J)$. The ferromagnetic configuration is nondegenerate, while the antiferromagnetic configuration is doubly degenerate, corresponding to two directions of the starting spin. The ground state energy remains unchanged if two of the bonds are ferromagnetic and two are antiferromagnetic. In all these cases, the directions of the spins can be easily chosen to satisfy the constraints imposed by the signs of the bonds, and the overall energy is minimized. However, the situation changes drastically if odd numbers of bonds are antiferromagnetic (Fig. 7c). One of the bonds then remains necessarily unsatisfied; the ground state energy is raised to $-2J$ and the degeneracy increases to eight, corresponding to two ways of choosing the direction of the initial spin and four ways of placing the unsatisfied bond. This simple illustration of frustration demonstrates how competing exchange interactions raise the ground state energy and degeneracy. Equivalent results are obtained even in the absence of competing interactions, provided one has structures that impose constraints leading to misfitting bonds. The simplest example is the two-dimensional triangular lattice with antiferromagnetically interacting Ising spins, a prob-

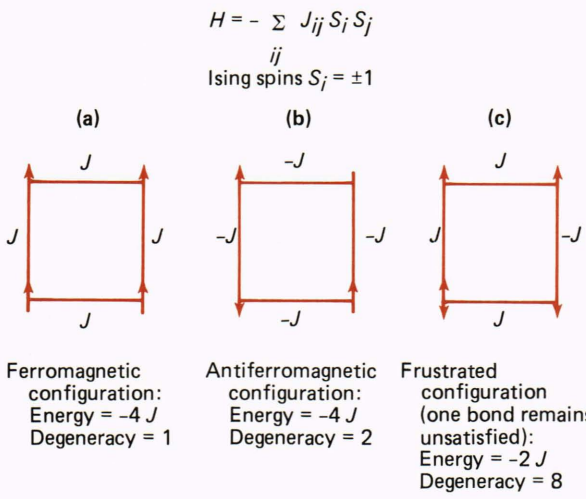

Figure 7—The Ising spins on a two-dimensional square lattice interacting via nearest-neighbor exchange interactions. The magnetic configuration, ground state energy obtained from the Hamiltonian H, and the degeneracy are shown for three cases. Note that in the frustrated configuration (3), the spin at the lower left-hand corner cannot simultaneously satisfy the instructions it gets from the two nearest neighbors.

lem studied long before the subject of spin glasses became important.[28] Its kinship to spin glasses lies in the observation that a disordered arrangement of atoms in an amorphous solid can lead to constraints that do not permit antiferromagnetic structure and consequently can lead to misfitted bonds.

The concept of frustration has proved to be a rich one. The importance of local symmetries in the model[27] and their relationship to lattice gauge field theories[29-31] previously introduced in connection with the quark confinement model[32,33] have been investigated. It is also proving useful in phenomena as varied as roughening transition in crystal growth theory,[34] orientation of complex molecules in solids,[35] incommensurate structures,[36] and content-addressable memory in neural networks.[37]

Broken Ergodicity and Ultrametric Topology

The large degeneracy or near-degeneracy in experimental examples of frustrated structures has led to the suggestion that the spin glass state is inherently nonergodic.[38] Many roughly equivalent free-energy minima with significant barriers between them exist (Fig. 8 shows a simplified version), so that some of the minima are inaccessible during the approach to equilibrium. Therefore, the system can get locked into a state of "local" equilibrium, in which the spin configurations and the consequent internal fields are quite different from those in the "true" equilibrium state. The system thus does not have the opportunity to sample the entire phase space and the ergodicity is said to be broken.[39]

Evidently, old order parameters (such as magnetization or sublattice magnetization) are of little use in the description of a glass phase characterized by mul-

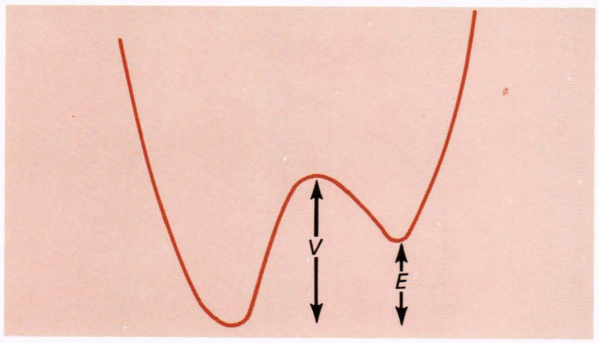

Figure 8—A simplified version of multiequilibrium states in spin glasses. The schematic shows two free-energy minima differing by an energy, E, and separated by a barrier height, V.

tiple energy states separated by barriers. To remedy this lacuna, a number of order parameters appropriate to the spin glass state have been suggested, the most general one being related to the probability distribution of the overlap of magnetizations between different states.[40]

A pure spin glass state, α, is characterized by the magnetization $m_j^\alpha \equiv \langle \sigma_j \rangle_\alpha$ at each site j with the angular brackets representing the thermodynamic average. The overlap, $q^{\alpha\beta}$, of two pure states α and β is defined as

$$q^{\alpha\beta} = \frac{1}{N} \sum_{j=1}^{N} m_j^\alpha \, m_j^\beta \,, \tag{2}$$

and the probability, $P_j(q)$, for a pair of states (α,β) to have an overlap q is given by

$$P_j(q) = \sum_{\alpha,\beta} P_\alpha P_\beta \, \delta(q - q^{\alpha\beta}) \,, \tag{3}$$

where P_α and P_β denote the weights of the pure states α and β. $P_q = \overline{P_J(q)}$ (the bar represents the average ove the exchange distribution) is normalized so that

$$\int_{-1}^{1} P(q) \, dq = 1.$$

Mézard et al.[41] show that the appropriate order parameter for the spin glass state is the probability distribution of $P_J(q)$ (which is already a probability distribution), whose fluctuations with respect to q do not vanish in the thermodyamic limit. The space of pure spin glass state has an ultrametric topology in that overlaps q_1, q_2, and q_3 between three pairs of any three pure states are such that at least two of them are equal and the third is larger than or equal to the other two (e.g., $q_1 \geq q_2 = q_3$). This leads to a hierarchical structure of the ensemble of spin glass states represented in Fig. 9 by a genealogical tree. The distance between two points on the tree is defined as the number of generations that separate them from a common ancestor. That the tree possesses ultrametric topology

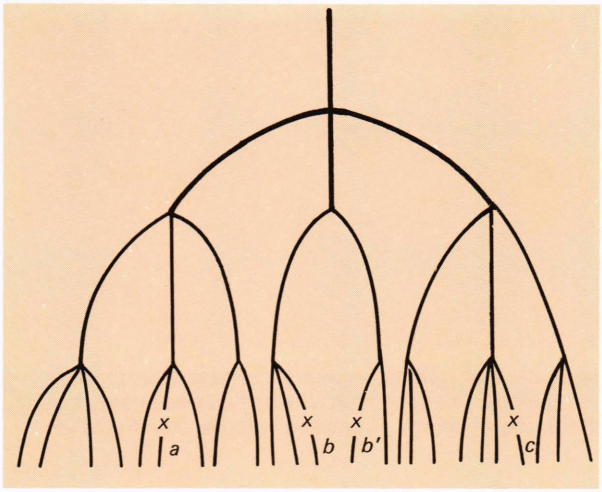

Figure 9—Ensemble of spin glass states represented by a hierarchical structure that exhibits ultrametric topology (see text).

is easily verified by cutting it at any ordinate and considering a set of any three points. For example, while points *a, b,* and *c* are all equidistant from their common ancestor for the set of points (b,b',c); *b* and b' are equidistant, while *c* is farther away. If end points denote states and the branches with all their descendents correspond to clusters, it is clear that for any value of q, if all the pure states that have overlaps larger than q are grouped together, the space of pure states is separated into disjointed clusters. The process can be continued by subdividing each cluster into smaller clusters. The picture therefore suggests a cascade of phase transitions. Such a cascade has also been suggested for ordinary glasses[42] and may indeed be characteristic of systems with broken ergodicity.

SPIN DYNAMICS

The dynamical behavior of spins in a broad class of spin glasses has been copiously investigated theoretically and experimentally. The materials of interest include metals, semiconductors, and insulators, and dilute as well as concentrated alloys, with spins situated either on a crystalline lattice or on an amorphous structure. A host of experimental techniques that include alternating-current susceptibility, magnetic resonance, positively charged muon spectroscopy, and neutron scattering has been employed to probe the spin dynamics. Much of the data have been reviewed in Chapter VII of Ref. 3.

The concern here is with spin dynamics in concentrated metallic spin glasses where direct exchange interactions, as opposed to indirect RKKY interactions, are expected to dominate. The prototype amorphous alloys that we have investigated include vapor-quenched Fe_xB_{100-x} and Mn_xB_{100-x} as well as liquid-quenched $(Fe_xNi_{1-x})_{75}(P\text{-}B\text{-}Al)_{25}$ and $(Fe_xNi_{1-x})_y(P\text{-}B)_{1-y}$. The choice of mostly iron-based alloys is due to the sensitivity of the sign of Fe-Fe exchange interaction to the Fe-Fe interatomic separation, which allows both ferro- and antiferromagnetic interactions to coexist in a certain compositional range. The amorphous atomic structure of the alloys implies that the frustration and the concomitant spin glass behavior originate not only from the competing exchange interactions, but also from the misfitting antiferromagnetic bonds on odd-membered structural rings.

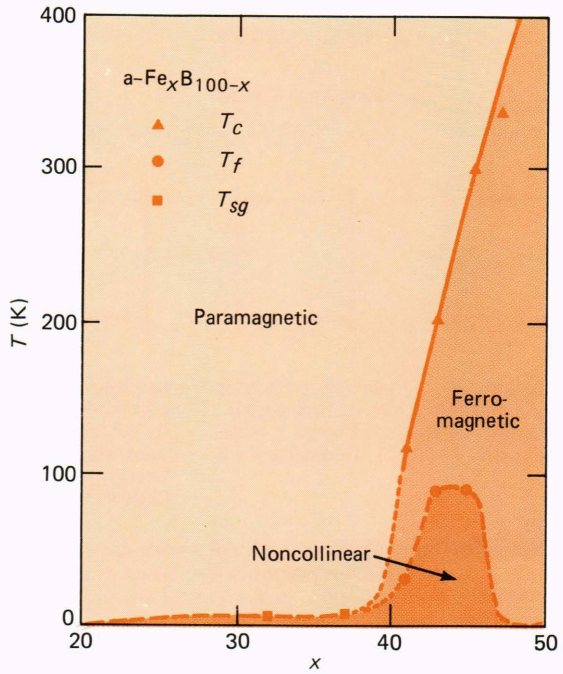

Figure 10—The magnetic phase diagram for amorphous Fe_xB_{100-x} alloys. As the temperature is reduced, alloys with $41 \leq x \leq 49$ show a paramagnetic-ferromagnetic phase transition at T_c followed by a transition at a lower temperature T_f to the noncollinear magnetic state from the ferromagnetic phase. Such alloys are referred to as reentrant alloys. Those with $x \leq 37$ enter the noncollinear magnetic phase directly from the paramagnetic state at T_{sg} and are called the spin glass alloys.

The magnetic phase diagram of the alloys under consideration, obtained from direct current measurements, is similar to that shown in Fig. 10 for a-Fe_xB_{100-x}.[43] As the system is diluted magnetically, conventional paramagnetic-ferromagnetic transition is observed at a Curie temperature, T_c, that decreases with decreasing composition, x, of the magnetic species. The decrease in T_c becomes more rapid as one approaches the multicritical point, x_m. For $x > x_m$, in a narrow range of composition, another transition from a ferromagnetic state to a frozen state is observed at T_f, with the transition line for all alloys except a-Fe_xB_{100-x} having a negative slope. For a-Fe_xB_{100-x}, T_f is a nonmonotonic function of x (Fig. 10). All such alloys are commonly referred to as reentrant alloys. For $x < x_m$, no ferromagnetism is observed, but a transition to a frozen state occurs directly from the paramagnetic phase, at a temperature T_{sg}. These alloys are normally referred to as spin glass alloys.

Below x_m, the magnetic behavior is dominated by the presence of finite magnetic clusters, while in the vicinity of x_m, an infinite ferromagnetic cluster and finite clusters coexist. Both intra- and intercluster in-

teractions are effective. A distribution of cluster sizes prevails, and one expects many different characteristic times associated with the dynamics of spins. In a random magnet, therefore, the dynamical phenomena lack a time scale,[5] and an adequate description necessarily involves many different techniques to explore various frequency domains. To monitor slow processes, one studies the time-dependence of thermoremanent magnetization and other history-dependent static response functions, e.g., susceptibility. For short-time behavior, however, one must use microscopic probes that include neutron scattering, muon spin relaxation, and electron spin resonance.[3]

Considering the complexities of the alloy systems of interest, one would expect that the spin relaxation rates as a function of magnetic composition, temperature, and frequency would be far from simple, except perhaps near a phase transition. Surprisingly enough, one of the main conclusions of our studies, derived mainly from spin resonance measurements[5,6] and supported by neutron scattering experiments, is that, in an enormous variety of random magnets, the spin relaxation rate exhibits a relatively simple temperature dependence, $(T/T_0)^n \exp(-T/T_0)$, where $n = 0$ or 1, and T_0 establishes the "scale" of temperature. It is remarkable that the behavior prevails over very wide ranges of temperature far removed from the transition temperatures T_f and T_{sg}.

Besides spin dynamics in reentrant and spin glass alloys, interest also lies in alloys within the concentration regime just above where reentrant behavior disappears. The latter regime is of importance because these alloys are not conventional ferromagnets but instead exhibit random characteristics in the sense that magnetic moments are not aligned in a specific direction. They thus exhibit noncollinear magnetic structures without the characteristics of a frozen state. The effect of such a behavior on spin dynamics is significant, as will be seen below.

Experimental Technique

The prime technique in our studies is that of spin resonance, which yields direct information on spin relaxation. The microwave absorption at fixed frequency is measured as a function of the magnetic field, and the resonance is characterized by the field for resonance and the line width. A systematic study usually involves measurements at several frequencies. In the materials of interest, the most important feature of the resonance is that the line shape remains unchanged over wide ranges of temperature. Thus the temperature dependence of the relaxation rate is reflected directly in the temperature variation of the observed line width.

As will be clearly demonstrated, the dynamical effects arise at temperatures far above the transition temperatures T_t (T_f or T_{sg}). Interest, therefore, is not just in the neighborhood of T_t; the random placement of spins has consequences far above T_t, and what appears as a paramagnetic or a ferromagnetic state at $T > T_t$ in static measurements is not a conventional paramagnetic or ferromagnetic state as probed by dynamical measurements.

The resonance line shape in amorphous alloys remains essentially unchanged over wide ranges of temperatures and frequencies and therefore the discussion of the line width, Γ, is equivalent to that of the relaxation frequency. Hence, only line width data are presented.

Paramagnets and Ferromagnets

For a conventional paramagnet, Γ depends linearly on temperature, $\Gamma = -a + bT$ (Bloch-Hasegawa behavior), and is approximately independent of the microwave frequency, ν. In a single crystal ferromagnetic alloy,[44] however, Γ is independent of temperature and proportional to ν. The Landau-Lifshitz-Gilbert equation of motion for the magnetization $\mathbf{M}$,

$$\dot{\mathbf{M}} = -\gamma\left[\mathbf{M} \times (\mathbf{H}_{eff} + \mathbf{H}_{int})\right] + \frac{\lambda}{\gamma M_s^2}\,\mathbf{M} \times \dot{\mathbf{M}}\,, \tag{4}$$

adequately describes the resonance in the presence of an applied field, $\mathbf{H}_{eff}$, that includes the static demagnetization field. In Eq. 4, M_s represents the saturation magnetization, λ is the frequency-independent damping parameter, and γ denotes the gyromagnetic ratio. Since for polycrystalline ferromagnets, in the absence of anisotropy, Γ is known to become temperature-independent for $T \leq 0.8\ T_c$, we define the ferromagnetic regime for the alloys under consideration as covering the range of temperature for which Γ is temperature-independent, and we discuss its frequency dependence. This contribution to the line width will be denoted by Γ_0. The absence of an exchange-conductivity contribution to Γ_0, which would arise if the exchange terms were included in Eq. 4, is justified by the typical resistivity values (approximately 1 microohm-meter) for the alloys of interest.

Random Magnets

In contrast to the above results on paramagnets and ferromagnets, the temperature and frequency dependences of Γ for reentrant and spin glass alloys are remarkably different. For example, in the reentrant a-$Fe_xNi_{80-x}P_{14}B_6$ alloys[45] (Fig. 11), while the ferromagnetic alloy ($x = 40$) does indeed show a temperature-independent line width, the line width rises at low temperatures as x is decreased ($x = 19, 17$), and—for alloys with $x \leq 15$—exhibits a low-temperature peak besides becoming temperature-dependent even at high temperatures. The various contributions are clearly separable as seen for the spin glass alloy[46] a-$Mn_{48}B_{52}$ in Fig. 12. The Bloch-Hasengawa behavior at high temperatures is followed by a temperature-independent component Γ_0 with a subsequent rise in Γ that starts at temperatures well above T_{sg}, followed by a peak located at $T < T_{sg}$. The observed frequency dependence of Γ is also shown. Note that lines through the

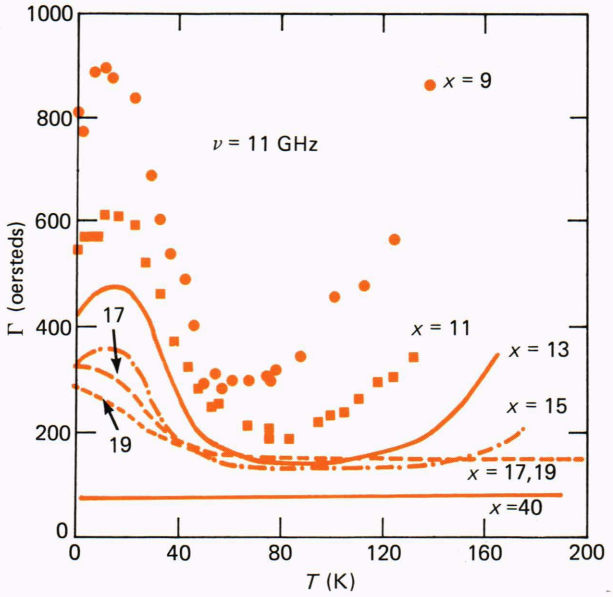

Figure 11—The temperature dependence of resonance line width in amorphous $Fe_xNi_{80-x}P_{14}B_6$ alloys. The alloy with $x = 40$ is ferromagnetic and exhibits a temperature-independent line width, while alloys with $9 \leq x \leq 19$ show reentrant behavior.

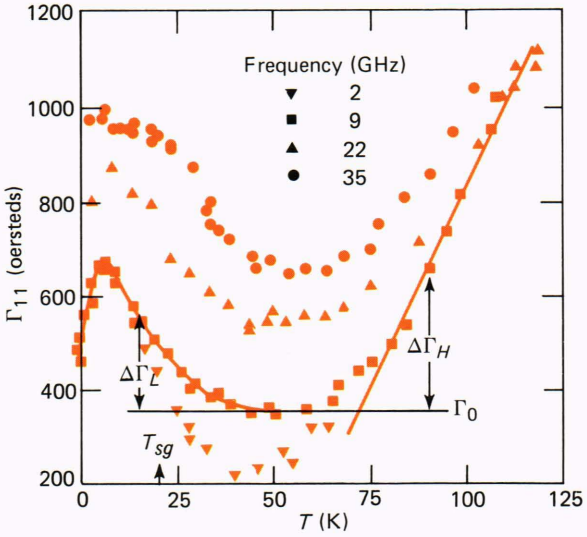

Figure 12—The variation of resonance line width with temperature in an amorphous $Mn_{48}B_{52}$ spin glass alloy at various frequencies. For the points at 9 gigahertz, the temperature-independent component Γ_0 and deviations from it at high ($\Delta\Gamma_H$) and low ($\Delta\Gamma_L$) temperatures are shown. The value of T_{sg} obtained from static measurements is shown by the arrow.

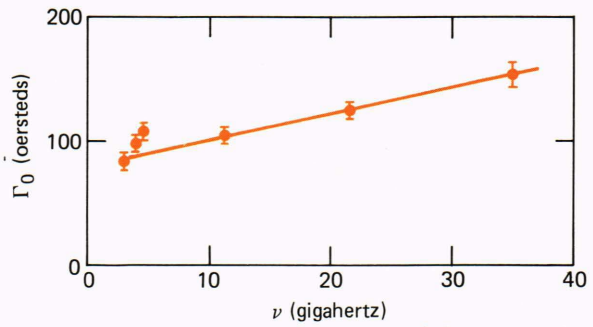

Figure 13—The frequency dependence of the temperature-independent component, Γ_0, of the resonance line width in the ferromagnetic amorphous $Fe_{51}B_{49}$ alloy. As expected for conventional ferromagnets, a linear frequency dependence is observed; however, in contrast to conventional ferromagnets, a finite intercept at zero frequency is seen.

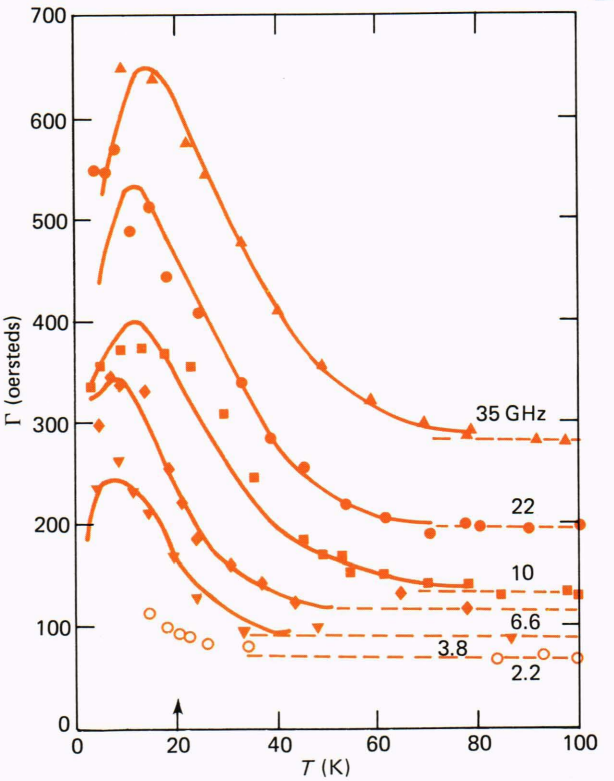

Figure 14—The variation of resonance line width with temperature in the reentrant amorphous alloy, $Fe_{15}Ni_{65}P_{14}B_6$, at various frequencies shown in gigahertz. The curves represent Eq. 5, with $n = 1$.

points (Figs. 11 and 12) are not just to guide the eye, but represent a particular functional dependence to be discussed later.

For ferromagnetic alloys, a-$Fe_{40}Ni_{40}P_{14}B_6$ (Fig. 11) and a-$Fe_{51}B_{49}$ (Fig. 13), Γ_0 is independent of temperature and proportional to frequency just as in crystalline ferromagnets. However, in contrast to crystalline ferromagnets, a finite line width results even at $\nu = 0$ (Fig. 13). This is also observed in reentrant[45] (a-$Fe_{13}Ni_{67}P_{14}B_6$, a-$Fe_{19}Ni_{56}P_{16}B_6Al_3$, a-$Fe_{30}Ni_{45}P_{16}B_6Al_3$) and spin glass[46] (a-$Mn_{48}B_{52}$, a-$Fe_7Ni_{73}P_{14}B_6$) alloys along with the increased Γ at high temperatures.

The full temperature and frequency dependence of the line widths is shown in Fig. 14 (also see Fig. 11) for typical reentrant alloys and in Fig. 15 (also see Fig. 12) for the spin glass alloys. In these figures the lines represent the expression

$$\Gamma = \Gamma_0 + \Gamma_1 (T/T_0)^n \exp(-T/T_0) , \qquad (5)$$

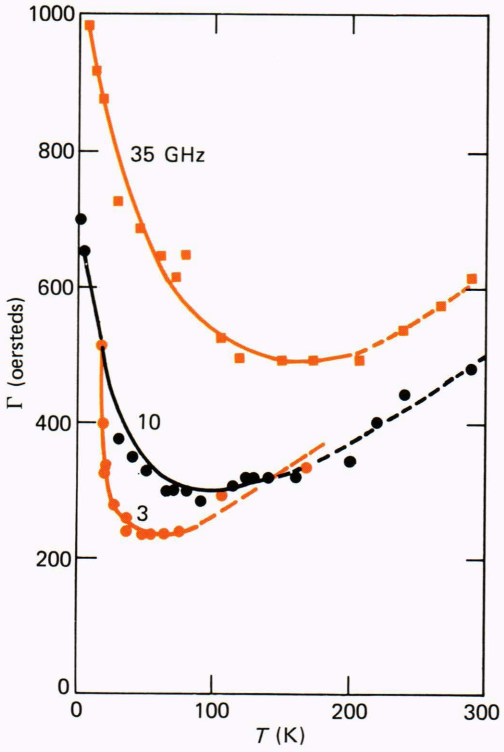

Figure 15—The temperature dependence of resonance line width in an amorphous spin glass alloy, FeB_2, at various frequencies. The curves represent Eq. 5, with $n = 0$.

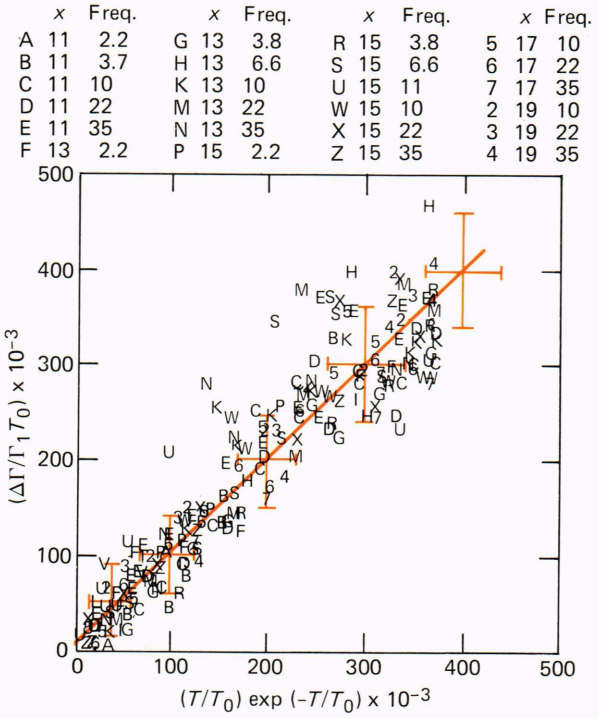

Figure 16—The universality plot (Eq. 5, with $n = 1$) for the reentrant amorphous metallic alloys, $Fe_xNi_{80-x}P_{14}B_6$. Note the large range of frequencies (in gigahertz) for which the data fall on the universal plot.

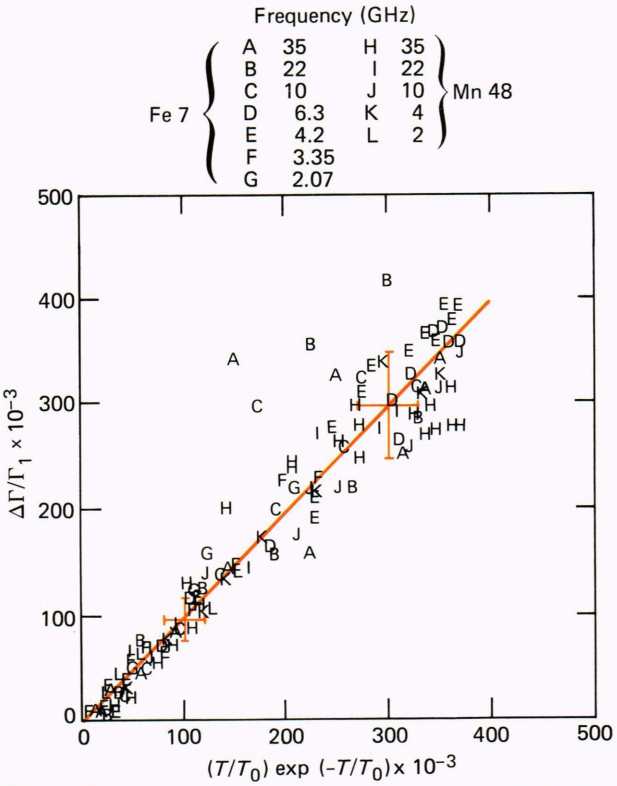

Figure 17—The universality plot (Eq. 5, with $n = 1$) for the amorphous metallic spin glass alloys, $Fe_7Ni_{73}P_{14}B_6$ and $Mn_{48}B_{52}$, at various frequencies.

with $n = 1$ in Figs. 11, 12, and 14 and $n = 0$ in Fig. 15. Except at the lowest temperatures in the highest frequency data ($\nu = 35$ gigahertz in Fig. 14), Eq. 5 reproduces the observed behavior extremely well. The determination of Γ_0 and Γ_1 from plots such as those shown in Figs. 11, 12, and 14 demonstrate the universal validity of Eq. 5 with $n = 1$ for a large body of data, over an extended range of temperatures and frequencies, in both reentrant (Fig. 16) and spin glass (Fig. 17) alloys. In fact, the dynamical behavior in an enormous number of random spin systems that include semimagnetic semiconductors,[47] dilute transition-metal/noble-metal alloys,[48] insulating alloys,[49] and amorphous metallic systems,[50] which exhibit the low-temperature rise in $\Delta\Gamma$, but not the peak at $T < T_f$, is well accounted for by Eq. 5 with $n = 0$ (Fig. 18).

A theoretical model, which may be appropriate to the universal behavior discussed above, is based on the interaction of magnetic excitations (e.g., spin waves in an infinite magnetic cluster) with the magnetic two-level systems considered to arise from finite magnetic clusters that act as relaxation channels for excitations in the infinite cluster.[51,52] The two-level systems, as already emphasized, are analogous to the tunneling centers in glasses[53] where the transitions occur, across a barrier height V, between two levels separated by an energy E (Fig. 8). For compact clusters and near the percolation threshold,[52] the barrier height distribution follows the exponential probability function $P(V) = 1/V_0 \exp(-V/V_0)$ and leads to Eq. 1 with $T_0 = V_0/\ln(w\tau_0)$, in the limits $w\tau_0 \ll 1$ and $kT/V_0 \ll 1$, where $\tau_0 \approx 10^{-13}$ seconds is the inverse of an

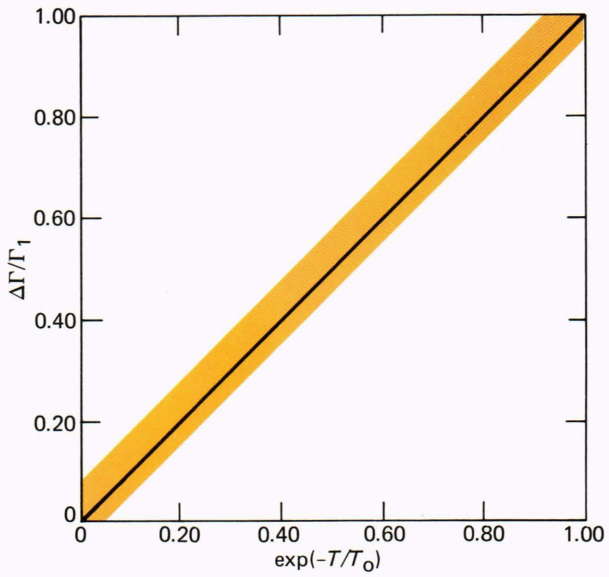

Figure 18—The universality plot (Eq. 5, with $n = 0$) for a large variety of alloys with randomly located spins.

attempt frequency. In this model, T_0 corresponds to the maximum in the line width and denotes the temperature at which the finite clusters freeze. Below T_0, the line width decreases since the frozen clusters are no longer efficient channels for excitations in the infinite cluster so that the lifetime of excitation modes increases. Though the overall observed behavior of Γ is reproduced by the model, since for $\omega/2\pi = 10$ gigahertz and $V_0 \approx 5\ kT_0$, the observed effects should occur at temperatures much below T_0, in contrast to the experimental data. Furthermore, as we have already noted, the same behavior is observed even in alloys where the transition to the noncollinear magnetic structure is from the paramagnetic state, where no infinite cluster exists.

Next, we mention the existence of a characteristic frequency, ν_c, for the spin glass alloys at which Γ rises far more rapidly with decreasing temperature than at frequencies below or above ν_c.[46] This is shown for a-$Mn_{48}B_{52}$ in Fig. 19 where $\nu_c = 4$ gigahertz. This resonant anomaly is observed for a number of spin glass alloys (Fig. 20) and strongly points to the presence of a high "density of states" local mode in the random spin systems.

Nonergodicity

Finally, we discuss a dynamic effect that is observed in the nonergodic behavior seen only in a-Fe_xB_{100-x} in a narrow concentration range,[19,43] $41 \leq x \leq 49$, of the reentrant alloys (Fig. 10) at all microwave frequencies. That these alloys differ from others was already remarked upon above, where it was noticed that the transition line between the ferromagnetic and the frozen state is nonmonotonic (Fig. 10). This is a result of the small size of boron atoms, which allows Fe-Fe atoms to approach each other closer than in other alloys, thus allowing a rapid change in the number of

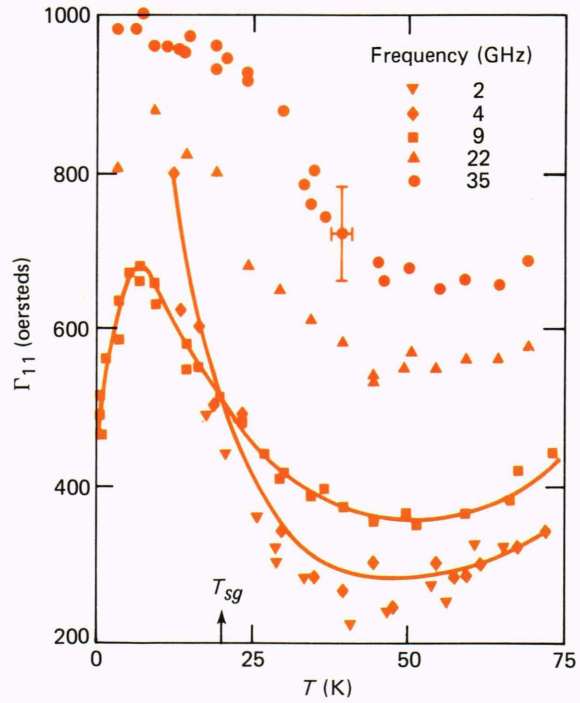

Figure 19—The resonance line width as a function of temperature in the amorphous spin glass alloy $Mn_{48}B_{52}$. Note that the low-temperature rise in the line width is sharper at 4 gigahertz than at frequencies below or above.

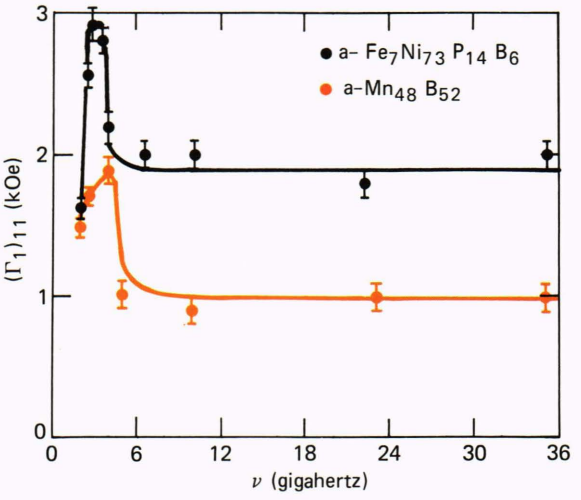

Figure 20—The frequency dependence of the line width in amorphous metallic spin glasses, $Fe_7Ni_{73}P_{14}B_6$ ($\nu_c = 3.4$ gigahertz) and $Mn_{48}B_{52}$ ($\nu_c = 4$ gigahertz).

antiferromagnetic bonds as a function of varying concentration. Considering Ising spins on a square lattice (Fig. 7), it is easy to demonstrate that the number of frustrated squares will initially increase with the increasing number of antiferromagnetic bonds, but will then decrease since it takes an odd number of antiferromagnetic bonds on an even-numbered ring to lead to frustration.[4,43] This has consequences in the static (Fig. 10) as well as dynamic (Fig. 21) behavior of the alloys. The line width γ as a function of concentration,

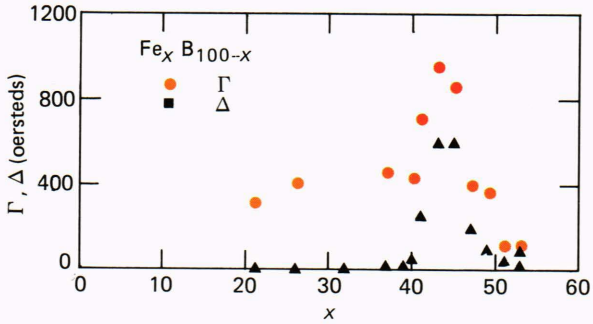

Figure 21—The concentration dependence of the resonance line width and the width of the hysteresis loop in amorphous Fe_xB_{100-x} alloys. The nonmonotonic behavior of Γ and Δ reflects the behavior of the transition temperature T_f seen in Fig. 10 and arises from the monotonicity of frustration as a function of antiferromagnetic bonds.

x, reflects the nonmonotonic behavior seen in Fig. 10 and furthermore follows the nonmonotonic variation of Δ, the width of the hysteresis loop.[43] More importantly, the nonergodic behavior is seen in Fig. 10 and furthermore follows the nonmonotonic variation of Δ, the width of the hysteresis loop.[43] More importantly, the nonergodic behavior is seen in Fig. 22, where the resonance field for a-$Fe_{49}B_{51}$ at $\nu = 12$ gigahertz in the parallel geometry has a temperature dependence that depends on the thermal history.[43] In the ferromagnetic regime ($T \geq 100$ K), the value of $H_\parallel$ is unique, but in the reentrant regime, $4\text{ K} < T < 100$ K, several paths result depending on the thermal cycling. The circles represent data taken while cooling from 300 K; the triangles and squares denote data obtained while warming, subsequent to cooling in zero field to 4 and 48 K, respectively. Note that the line width (the upper part of Fig. 22) is essentially independent of the path. Similar behavior is seen in other reentrant alloys ($41 \leq x \leq 49$) and at various frequencies. We ascribe it to nonergodicity.[19,43] The free energy for the spin glass phase, as noted earlier, exhibits a large number of quasi-degenerate minima separated by barriers of varying heights (a generalized version of the two-level system in Fig. 8). It is then possible that the spin system gets "locked" into a metastable state and is unable to "visit" the other minima. In each of the equivalent many-spin configurations, the angular dependences of the local energies are expected to be different, so that they will represent a variety of local anisotropy fields.

CONCLUSIONS

The spin resonance measurements have clearly demonstrated that the effects of transitions to the noncollinear magnetic phases are felt at temperatures far above the transition temperature obtained from the static measurements. The temperature and frequency dependence of the resonance line width and field have revealed a variety of dynamical phenomena that include universality, the existence of characteristic frequencies, and nonergodicity. It is well established that random systems do not possess a unique length scale;[54] resonance

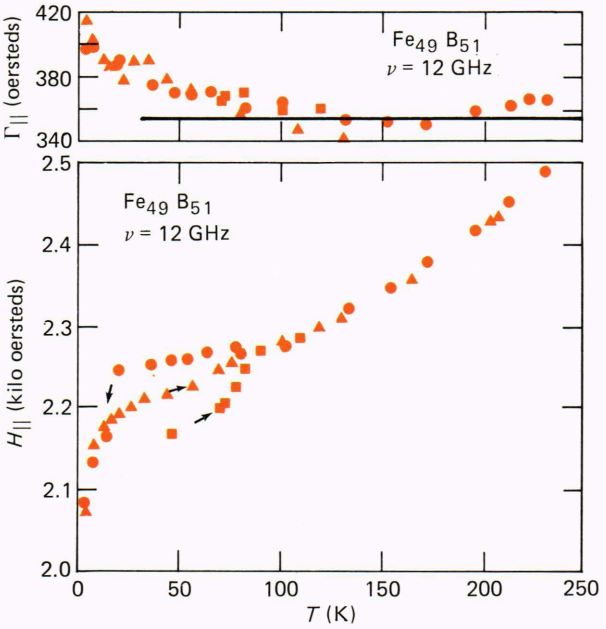

Figure 22—The temperature dependence of line width (top) and resonance field (bottom) in the amorphous reentrant alloy $Fe_{49}B_{51}$. The nonergodic behavior observed during thermal cycling is discussed in the text.

data establish the absence of a time scale, for dynamics of spins, in random media.

EPILOG

The research described in this article has dealt at some length with the dynamics of spin of random magnets. Recent studies have also focused on atomic structure, static magnetization measurements using a superconducting quantum interference device magnetometer, and high-resolution electrical transport measurements on vapor- and liquid-quenched alloys.[55-57] The relationship between the microstructure and the magnetic and transport properties of liquid-quenched $Fe_{60}Al_{28}B_{12}$ alloys, which are of interest from the structural and corrosion point of view, has been delineated.[55] Future interests lie in the area of controlling the nonergodic behavior of reentrant alloys by compositional modification for possible uses in magnetic content-addressable memories and the problem of magnetic recording in alloys with perpendicular anisotropy.

REFERENCES

[1] *Magnetic Materials,* NMAB Report No. 426, National Academy Press, Washington, D.C. (1985).
[2] S. M. Bose, K. Moorjani, T. Tanaka, and M. M. Sokoloski, *Amorphous Magnetism*, H. O. Hooper and A. M. deGraaf, eds., Plenum Press, New York, p. 421 (1973).
[3] K. Moorjani and J. M. D. Coey, *Magnetic Glasses,* Elsevier Science Publishers, Amsterdam (1984).
[4] K. Moorjani, in *Physics of Disordered Materials,* D. Adler, H. Fritzsche, and S. R. Ovshinsky, eds., Plenum Press, New York, p. 699 (1985).
[5] K. Moorjani, S. M. Bhagat, and M. A. Manheimer, *Transport and Relaxation Processes in Random Materials,* World Science Publishers (in press).
[6] K. Moorjani, S. M. Bhagat, and M. A. Manheimer, *IEEE Trans. Magn.* (in press).
[7] V. Jaccarino and L. R. Walker, *Phys. Rev. Lett.* **15**, 258 (1965).
[8] G. Marchal, D. Teirlinck, P. Mangin, C. Janot, and J. Hübsch, *J. Phys.* **41**, C8-662 (1980).

[9]N. A. Blum, K. Moorjani, T. O. Poehler, and F. G. Satkiewicz, *J. Appl. Phys.* **52**, 1808 (1981); **53**, 2074 (1982).
[10]D. W. Forrester, N. C. Koon, J. H. Schelleng, and J. J. Rhyne, *J. Appl. Phys.* **50**, 7336 (1979).
[11]R. Harris, M. Plischke, and M. J. Zuckerman, *Phys. Rev. Lett.* **31**, 160 (1973).
[12]A. B. Harris, *J. Phys.* **C7**, 1671 (1974).
[13]K. Handrich, *Phys. Status Solidi* **32**, K55 (1969).
[14]H. Falk and G. A. Gehring, *J. Phys.* **C8**, L298 (1975).
[15]K. Moorjani and S. K. Ghatak, *J. Phys.* **C10**, 1027 (1977).
[16]F. Bloch, *Z. Phys.* **61**, 206 (1930); **74**, 295 (1932).
[17]L. D. Landau and E. M. Lifshitz, *Phys. Z. Sowjetunion* **8**, 153 (1935).
[18]R. W. Cochrane and G. S. Cargill III, *Phys. Rev. Lett.* **32**, 476 (1974).
[19]D. J. Webb, S. M. Bhagat, K. Moorjani, T. O. Poehler, and F. G. Satkiewicz, *Solid State Commun.* **43**, 239 (1982).
[20]D. T. Pierce, R. J. Celotta, J. Unguris, and H. C. Siegman, *J. Magn. Magn. Mater.* **35**, 28 (1983).
[21]D. L. Mills and A. A. Maradudin, *J. Phys. Chem. Solids* **28**, 1855 (1967).
[22]V. Cannela, J. A. Mydosh, and J. I. Budnick, *J. Appl. Phys.* **42**, 1689 (1971).
[23]R. J. Borg, *Phys. Rev.* **B1**, 349 (1970).
[24]A. Arrott, *J. Appl. Phys.* **35**, 1093 (1965).
[25]S. F. Edwards and P. W. Anderson, *J. Phys.* **F5**, 965 (1975).
[26]K. Moorjani and J. M. D. Coey, *Magnetic Glasses,* Chap. 3, Elsevier Science Publishers, Amsterdam (1984).
[27]G. Toulouse, *Commun. Phys.* **2**, 115 (1977).
[28]G. H. Wannier, *Phys. Rev.* **79**, 357 (1950); also see errata, *Phys. Rev.* **B7**, 5017 (1973).
[29]E. Fradkin, B. A. Huberman, and S. H. Shenker, *Phys. Rev.* **B18**, 4789 (1978).
[30]G. Toulouse and J. Vannimenus, *Phys. Rep.* **67**, 47 (1980).
[31]J. A. Hertz, *Phys. Rev.* **B18**, 4875 (1978).
[32]K. G. Wilson, *Phys. Rev.* **D10**, 2445 (1974).
[33]R. Balian, J. M. Drouffe, and C. Itzykson, *Phys. Rev.* **D10**, 3376 (1974).
[34]G. Toulouse, J. Vannimenus, and J. M. Maillard, *J. Physique Lett.* **38**, L459 (1977).
[35]F. Borsa, U. T. Höchli, J. J. van der Klink, and D. Rytz, *Phys. Rev. Lett.* **45**, 1884 (1980).
[36]S. Aubry, *Ferroelectrics* **24**, 53 (1980).
[37]J. J. Hopfield, in *Proc. Nat. Acad. Sci.* **79**, 2554 (1982).
[38]P. W. Anderson, in *La Matiere Mal Condensé-Ill – Condensed Matter,* R. Balain, R. Maynard, and G. Toulouse, eds., North-Holland, Amsterdam, 159 (1979).
[39]R. G. Palmer, *Adv. Phys.* **31**, 669 (1982).
[40]G. Parisi, *Phys. Rev. Lett.* **50**, 1946 (1983).
[41]M. Mézard, G. Parisi, N. Sourlas, G. Toulouse, and M. Virasoro, *Phys. Rev. Lett.* **52**, 1156 (1984).
[42]R. G. Palmer, D. L. Stein, E. Abrahams, and P. W. Anderson, *Phys. Rev. Lett.* **53**, 958 (1984).
[43]D. J. Webb, S. M. Bhagat, K. Moorjani, T. O. Poehler, F. G. Satkiewicz, and M. A. Manheimer, *J. Magn. Magn. Mater.* **44**, 158 (1984).
[44]I. M. Puzei and V. C. Pokatilov, *Solid State Phys.* (Soviet Union) **16**, 671 (1974); also see S. M. Bhagat and P. Lubitz, *Phys. Rev.* **B10**, 179 (1974), and L. Kraus, Z. Frait, and J. Schneider, *Phys. Status Solidi* (*a*) **63**, 669 (1981).
[45]S. M. Bhagat, D. J. Webb, and M. A. Manheimer, *J. Magn. Magn. Mater.* **53**, 209 (1985).
[46]M. J. Park, S. M. Bhagat, M. A. Manheimer, and K. Moorjani, *Phys. Rev.* **B33**, 2070 (1986); *J. Magn. Magn. Mater.* **54-57**, 109 (1986).
[47]S. M. Bhagat and H. A. Sayad, *J. Magn. Magn. Mater.* (to be published); S. Oseroff, *Phys. Rev.* **B25**, 6584 (1982).
[48]G. Mozurkewich, J. H. Elliott, M. Hardiman, and R. Orbach, *Phys. Rev.* **B29**, 278 (1984).
[49]J. P. Jamet, J. C. Dumais, J. Seiden, and K. Knorr, *J. Magn. Magn. Mater.* **15-18**, 197 (1980); D. Fiorani, S. Viticoli, J. L. Dorman, J. L. Tholence, and A. P. Murani, *Phys. Rev.* **B30**, 2776 (1984); S. Viticoli, D. Fiorani, M. Nognas, and J. L. Dorman, *Phys. Rev.* **B26**, 6085 (1982).
[50]K. Moorjani, T. O. Poehler, F. G. Satkiewicz, M. A. Manheimer, D. J. Webb, and S. M. Bhagat, *J. Appl. Phys.* **57**, 3444 (1985).
[51]M. A. Continentino, *Phys. Rev.* **B27**, 4351 (1983); *J. Phys. C: Solid State Phys.* **16**, L71 (1983).
[52]M. H. Cohen and M. A. Continentino, *Solid State Commun.* **55**, 609 (1985).
[53]P. W. Anderson, B. I. Halperin, and C. M. Varma, *Phil. Mag.* **25**, 1 (1972); W. A. Phillips, *J. Low Temp. Phys.* **7**, 351 (1972).
[54]B. B. Mandelbrot, *Fractals: Form, Chance, and Dimension,* Freeman, San Francisco (1977); also see various papers in Ref. 4.
[55]T. J. Kistenmacher, W. A. Bryden, and K. Moorjani, *J. Magn. Magn. Mater.* **54-57**, 1611 (1986).
[56]W. A. Bryden, J. S. Morgan, T. J. Kistenmacher, and K. Moorjani, *Bull. Am. Phys. Soc.* **31**, 285 (1986).
[57]K. Moorjani, W. A. Bryden, and T. J. Kistenmacher, *Bull. Am. Phys. Soc.* **31**, 284 (1986).

ACKNOWLEDGMENTS—I owe a debt of gratitude to my many collaborators who have made substantial contributions to the research described here. Among them are: N. A. Blum, W. A. Bryden, K. Hoggarth, T. J. Kistenmacher, J. W. Leight, J. S. Morgan, T. O. Poehler, and F. G. Satkiewicz at APL; S. M. Bhagat at the University of Maryland; J. M. D. Coey of Trinity College, Dublin; S. K. Ghatak at the Indian Institute of Technology, Kharagpur, and Freie Universität, West Berlin; M. A. Manheimer of the Laboratory for Physical Sciences; M. J. Park of the Korea University; and D. J. Webb at Stanford University. Partial support for this research has been provided by the Naval Sea Systems Command, U. S. Department of the Navy, and in initial stages by the Army Research Office, Durham, and at various times by the Centre National de la Recherche Scientifique, France.

THE AUTHOR

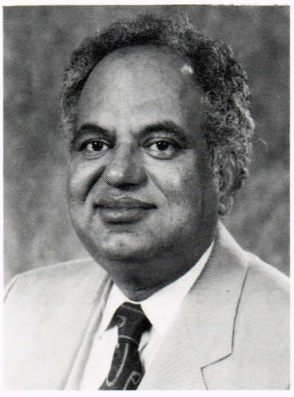

KISHIN MOORJANI is a physicist in APL's Materials Research Group engaged in problems related to artificially structured materials. Born in India, he studied at the University of Delhi and the University of Maryland before receiving his Ph.D. degree in physics at The Catholic University of America in 1964. In 1967, Dr. Moorjani joined APL, where he is currently program manager of the Microphysics project. He has co-authored a monograph, *Magnetic Glasses*, and has published extensively in the field of condensed matter sciences. He has held several visiting appointments at universities both in the United States and abroad. Dr. Moorjani teaches in Johns Hopkins' G.W.C. Whiting School of Engineering Part-Time Programs and serves on the University's Applied Physics Program Committee.